Hot pressing and spark plasma sintering of alumina: Discussion about an analytical modelling used for sintering mechanism determination

P. Guyot,[a] G. Antou,[a,*] N. Pradeilles,[a] A. Weibel,[b] M. Vandenhende,[a] G. Chevallier,[b] A. Peigney,[b] C. Estournès[b] and A. Maître[a]

[a]*SPCTS, UMR CNRS 7315, Centre Européen de la Céramique (CEC), 12 rue Atlantis, 87068 Limoges Cedex, France*
[b]*Institut Carnot CIRIMAT, UMR CNRS 5085, 118 route de Narbonne, 31062 Toulouse Cedex 09, France*

The validity of the model for sintering under uniaxial pressure proposed by Bernard-Granger et al. has been investigated by studying the densification kinetics of a submicrometric α-alumina powder using hot pressing and spark plasma sintering devices. The identified key parameters of creep (i.e. stress exponent, apparent activation energy) seem to be unreliable, and do not in the end allow identification of the involved sintering mechanism. Possible biases of the approach are identified and discussed.

Keywords: Ceramics; Spark plasma sintering; Hot pressing; Modelling; Densification

Hot pressing (HP) and spark plasma sintering (SPS) are very widespread pressure-assisted sintering techniques, both of which are used in ceramics, metals and composites engineering. These techniques usually involve a uniaxial press coupled with a heating device, and are known to allow the manufacturing of fully dense materials at lower temperatures and shorter cycle times than conventional techniques. The main difference between HP and SPS rests on the heating system: in HP, the sample is heated by a radiative furnace, whilst in SPS, the Joule effect caused by a pulsed direct current (typically a few thousand amperes and a few volts) provides the primary heating source. However, divergent analyses of SPS mechanisms have been reported in a recent viewpoint set [1].

To understand fully the mechanisms involved in pressure-assisted sintering, analytical models have been developed and transposed to SPS in order to highlight potential discrepancies between SPS and HP. These discrepancies could arise from the existence of possible specific effects during SPS. This paper focuses on the analytical model recently suggested by Bernard-Granger and Guizard [2] that allows the densification mechanism to be identified in a relatively simple manner. This approach has been applied to several ceramic systems [2–7], including α-Al_2O_3 [6]. It is based on the steady-state creep model established by Mukherjee et al. [8] to describe the creep of dense materials, and thus assumes that the main driving force of pressure-assisted sintering is due to the macroscopic applied pressure; this model neglects the contributions from pressure-less sintering and, in the case of SPS, the specific effects that can occur such as electromigration [9], electromagnetic effect [10] or thermal diffusion due to possible high local temperature gradients [11].

The dependence of the normalized densification kinetics on temperature, applied stress and microstructural evolution is expressed as follows:

$$\frac{1}{\mu_{\text{eff}}}\frac{1}{D}\frac{dD}{dt} = K\frac{e^{\frac{-Q_d}{RT}}}{T}\left(\frac{b}{G}\right)^p\left(\frac{\sigma_{\text{eff}}}{\mu_{\text{eff}}}\right)^n, \quad (1)$$

where D is the instantaneous relative density, K is a constant, G is the grain size, σ_{eff} is the instantaneous effective stress acting on the powder bed and μ_{eff} is the instantaneous shear modulus of the powder bed, t is

* Corresponding author. Tel.: +33 (0)5 87 50 23 97; fax: +33 (0)5 87 50 23 04; e-mail: guy.antou@unilim.fr

http://dx.doi.org/10.1016/j.scriptamat.2014.04.013

the time, b is the Burgers vector, R is the ideal gas constant, Q_d is the apparent activation energy of the mechanism controlling the densification, and p and n are the exponents for grain size and stress, respectively.

This approach is based on the assessment of the instantaneous effective stress σ_{eff} acting on the powder bed using the geometric model developed by Helle et al. for relative density values up to 0.9 during hot isostatic pressing treatments [12]:

$$\sigma_{eff} = \frac{1 - D_0}{D(D - D_0)} \sigma_{\text{mac}}, \tag{2}$$

where σ_{mac} is the macroscopic uniaxial pressure applied to the powder bed and D_0 is the green density.

The instantaneous effective shear modulus μ_{eff} is calculated according to the empirical relation suggested by Lam et al. [13] to describe the elasticity of porous alumina sintered ceramics:

$$\mu_{\text{eff}} = \frac{E_{\text{th}}}{2(1 + \nu_{\text{eff}})} \frac{D - D_0}{1 - D_0}, \tag{3}$$

where ν_{eff} is the effective Poisson's ratio and E_{th} is the Young's modulus of the theoretically dense material.

In the present work, this analytical approach is studied and discussed considering both the densification by HP and SPS of a commercially submicrometric alumina powder.

All HP experiments were carried out on a Goliath Graphite 2000 (La Physique Appliquée, France). The SPS apparatus used was a Dr. Sinter 2080 (Fuji Electronics Industrial Co. Ltd., Japan). The ceramic material used was an α-Al_2O_3 powder, 99.99% pure, with a median particle size of 140 nm (TM-DAR, TaiMei Chemicals, Japan).

For both experiments, 2.5 g of powder was poured into a graphite die with an inner diameter of 20.4 mm. A compressible graphite foil (0.2 mm thick, Papyex®, Mersen, France) was used as lubricant to coat the inner surface of the die and the surface of the punches. The same die geometry was used in both cases to allow a better comparison between the results obtained on the HP and SPS devices.

According to the literature [14,15], significant temperature gradients can occur in SPS devices. Consequently, calibration experiments were conducted to measure the discrepancy between the temperature measured by the pyrometer on the die side and the actual temperature determined by a thermocouple buried into the alumina powder. The actual temperatures of the powder so obtained were taken into account when apply the analytical model. In the HP apparatus, a previous calibration test was conducted to obtain the actual temperature.

With the HP device, tests were performed at different temperatures (900, 950 and 1000 °C), under an applied stress of 20, 35, 42.5 and 50 MPa. The heating rate was 15 °C min^{-1}, and the dwell time was 60 min (see Fig. 1). With the SPS device, tests were performed at similar temperatures (950, 1000 and 1050 °C), under an applied stress of 35, 42.5 and 50 MPa. Here, the heating rate was 100 °C min^{-1}, and the dwell time was 15 min. In the case of SPS treatments, the temperatures measured by the pyrometer were on average underestimated by 60 °C on the dwell, according to the calibration test. In both cases, the displacement was recorded by the device, and for each experiment, a blank cycle was performed by submitting a fully dense pellet to a complete heating cycle, in order to remove the dilatation of the die, punches and alumina from the recorded data.

The relative density of the sintered samples was measured using geometrical measurements and the Archimedes method. The initial green density was then calculated using the displacement curve. The Young's modulus of fully dense alumina was determined using ultrasonic sounding.

The evolution of the relative density on the isothermal dwell was calculated from the recorded axial displacement via the following expression (see Fig. 1):

$$D = D_f \cdot \frac{h_f}{h}, \tag{4}$$

where D is the relative density, D_f is the final relative density (measured by the Archimedes method), h_f is the final height of the sample and h is the instantaneous height of the sample.

To identify the creep parameters (i.e. stress exponent and apparent activation energy values), the evolution of the sintering kinetics is studied in isothermal and isobar regimes without the occurrence of grain growth, as shown in Figure 2a,b for the selected limit sintering conditions.

In order to determine the effective stress exponent n following the proposed approach by Bernard-Granger and Guizard [2], the curves giving $\ln\left[\frac{1}{\mu_{\text{eff}}} \frac{1}{D} \frac{dD}{t}\right]$ as a function of $\ln\left(\frac{\sigma_{\text{eff}}}{\mu_{\text{eff}}}\right)$ were plotted from the whole dataset obtained continuously throughout the isothermal dwells. This relation is supposed to lead to a linear law the slope of which gives the value of the stress exponent n.

As shown in Figure 3a,c, this relation is not linear if the entire dwell time is considered. The instantaneous value of n has been calculated for each value of the density (Fig. 3b,d) and shows a continuous variation of this exponent throughout the isothermal stage of sintering. It suggests a continuous evolution of the sintering mechanism, which seems to be unlikely.

Moreover, for several experiments at the end of the dwell, n increases up to ~11. A high value of n normally corresponds to creep mechanism controlled by dislocation motion ($n > 3$). It should be noted that for the same experimental conditions in SPS, Santanach et al. have shown that no dislocation can be observed within the microstructure of the sintered material [6], which means these mechanisms are unlikely to occur. The restricted existence of this power-law creep regime is in accordance with the hexagonal structure of α-alumina which has few active slip systems. Moreover, these really high values of n have no physical sense. As a matter of fact, in the case of iono-covalent ceramics such as alumina-based ceramics, power-law creep can be normally correlated to a maximum stress exponent value of ~5, because plastic flow related to the intragranular motion of dislocations is limited by: (i) the low density of dislocations and by their low mobility linked to the existence of high Peierls stress; (ii) the restricted slip systems for homogeneous

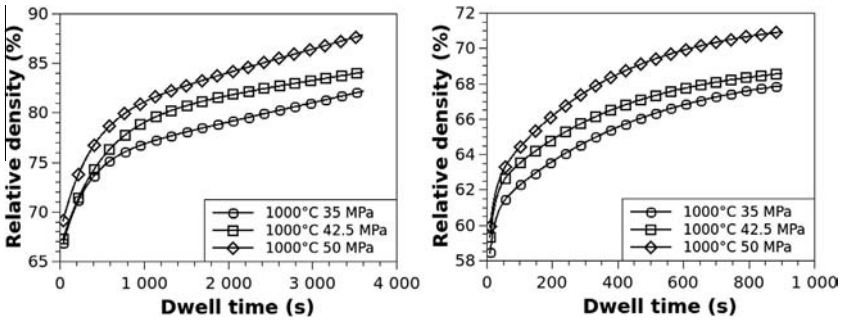

Figure 1. Evolution of the relative density under isothermal conditions: (a) HP; (b) SPS.

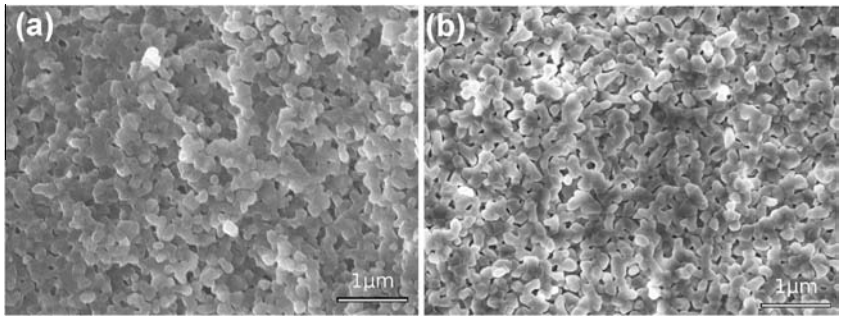

Figure 2. Field emission gun scanning electron microscopy observations of the samples; (a) HP sintered at 1000 °C under 50 MPa (relative density = 87%); (b) SPS sintered at 1050 °C under 50 MPa (relative density = 81%).

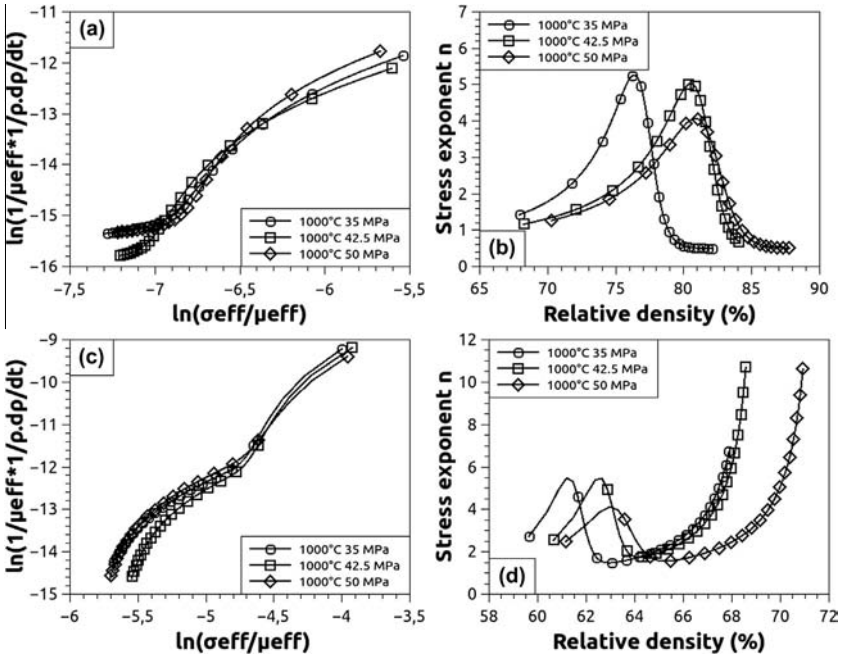

Figure 3. Determination of the effective stress exponent during isothermal dwells: (a,b) HP; (c,d) SPS.

plastic deformation; and (iii) low grain size typically encountered in ceramics linked to their low grain-boundary mobilities compared to metals [16].

According to Bernard-Granger and Guizard [2], the apparent activation energies are calculated for a fixed value of the normalized densification rate of $2.3 \times 10^{-5}\,s^{-1}$ in HP and $5.0 \times 10^{-5}\,s^{-1}$ in SPS (Fig. 4). For a given value of n, the activation energy values so determined seem similar for HP and SPS. However, a strong dependence of the considered stress exponent value on the calculated apparent activation energies appears to exist. It can be seen that when the stress exponent value ranges from 1 and 2, the determined activation energy is multiplied by a factor of

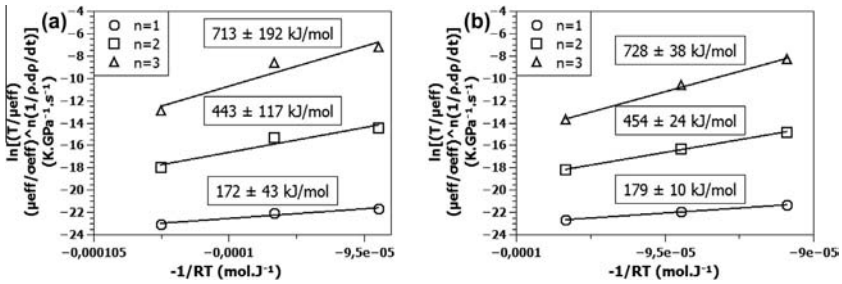

Figure 4. Determination of the apparent activation energy for several values of n: (a) HP; (b) SPS.

2.5. Consequently, the apparent activation energy cannot be evaluated following this methodology.

Several reasons can explain the bias of this approach. Firstly, the determined creep parameters strongly depend on precise evaluations of: (i) the effective shear modulus using the empirical model suggested by Lam et al. [13]; (ii) the instantaneous effective stress which is based on the geometrical model developed by Helle et al. [12]. This latter model has been developed for single-sized spherical powders close to a random dense stacking during hot isostatic pressing. It might not apply to loose powders submitted to a uniaxial stress during sintering, especially if the powders are not spherical.

Secondly, the model is strongly dependent on the initial density of the powder material, and any uncertainty in this value can lead to dramatic uncertainties in the value of the stress exponent as suggested in Ref. [6]. Indeed, it is hard to determine precisely the initial powder density, especially if the loose powder has been poured into the die without a pre-compacting step. The initial density has to be calculated by using both the final density of the sintered pellet and the densification curve. Even if a pellet is put into the die instead of loose powder, the uniaxial pressure is likely to increase its initial density, resulting in a bias in the value of the green density.

Lastly, this model does not take into account the radial and tangential stresses, which can be generated by the thermal expansion mismatch between the material and the die, and by the radial thermal gradients. It has been shown by finite-element simulation that the contribution of these components of the stress tensor can be significant [15]. Plastic flow of the porous body is related to the effective stress acting on the powder bed, which is a combination of deviatoric and hydrostatic parts of the stress field [17].

In this work, the pressure-assisted sintering model suggested by Bernard-Granger et al. has been applied to a submicrometric α-alumina powder sintered by HP and SPS. From the analysis of densification kinetic data using this approach, the identified creep parameters seem to be unreliable. Even if the applied approach is attractive due to the limited number of experiments needed to study the sintering mechanism, the main possible reasons for the bias of the approach are: (i) the strong dependence of the determined creep parameters on precise evaluations of the effective stress acting on the powder bed and of the effective shear modulus; and (ii) neglecting the radial and tangential thermally generated stresses.

Consequently, a creep investigation which consists in analysing kinetics evolution in isothermal and isobar conditions for a fixed microstructure should be preferred to obtain reliable creep parameters. In a companion study to be published, we will suggest a new approach to identify sintering mechanisms without having to evaluate the effective stress acting on the powder bed. This approach will be justified by a continuum micromechanical model that integrates the entire stress field; this will be used to compare HP and SPS.

This work was carried out within the IMPULSE project thanks to the financial support of the French National Research Agency (ANR).

[1] S.H. Risbud, Y.-H. Han, Scripta Mater. 69 (2) (2013) 105–206.
[2] G. Bernard-Granger, C. Guizard, Acta Mater. 55 (2007) 3493–3504.
[3] G. Bernard-Granger, A. Addad, G. Fantozzi, G. Bonnefont, C. Guizard, D. Vernat, Acta Mater. 58 (2010) 3390–3399.
[4] G. Bernard-Granger, N. Benameur, A. Addad, M. Nygren, C. Guizard, S. Deville, J. Mater. Res. 24 (6) (2009) 2011–2020.
[5] M. Gendre, A. Maître, G. Trolliard, Acta Mater. 58 (2010) 2598–2609.
[6] J. Santanach, A. Weibel, C. Estournès, Q. Yang, C. Laurent, A. Peigney, Acta Mater. 59 (2011) 1400–1408.
[7] G. Bernard-Granger, C. Guizard, J. Mater. Res. 24 (1) (2009) 179–186.
[8] A. Mukherjee, J. Bird, J. Dorn, Trans. Am. Soc. Met. 62 (1969) 155–179.
[9] E.A. Olevsky, L. Froyen, Scripta Mater. 55 (2006) 1175–1178.
[10] P. Guyot, V. Rat, J.F. Coudert, F. Jay, A. Maître, N. Pradeilles, J. Phys. D Appl. Phys. 45 (9) (2012) 92001–92004.
[11] E.A. Olevsky, L. Froyen, J. Am. Ceram. Soc. 92 (S1) (2009) S122–S132.
[12] A.S. Helle, K.E. Easterling, M.F. Ashby, Acta Metall. 33 (12) (1985) 2163–2174.
[13] D. Lam, F. Lange, A. Evans, J. Am. Ceram. Soc. 77 (1994) 2113–2117.
[14] U. Anselmi-Tamburini, S. Gennari, J.E. Garay, Z.A. Munir, Mater. Sci. Eng., A 394 (2005) 139–148.
[15] G. Antou, G. Mathieu, G. Trolliard, A. Maître, J. Mater. Res. 24 (2009) 404–412.
[16] R.W. Cannon, T.G. Langdon, J. Mater. Sci. 23 (1988) 1–20.
[17] R.J. Green, Int. J. Mech. Sci. 14 (1972) 2.